M.T. Yassen
Microwave Research Group, Department of Electrical Engineering, University of Technology, Baghdad, Iraq
mahmoud_alanssary@yahoo.com

Received on: 14/04/2016
Accepted on: 18/08/2016

A New Compact Dual-band Antenna Based on Sierpinski Curve Slotted Ground Plane and Current Distribution Analysis

Abstract- *A new design approach has been used to achieve a dual band response from a multi-band resonance. The design approach is wholly depending on current distribution analysis on the surface of a multi-band antenna. The proposed multi-band antenna consists of a slotted ground plane with a simple 50-ohm microstrip feed line on the other side of an FR4 substrate having 4.4 relative dielectric constant and 1.6 mm thickness. The geometry of the first iteration Sierpinski curve fractal has been employed to the slotted ground plane antenna structure. Two small squares have been inserted to both internal upper corners of the slotted ground plane as a technique to control the path of electrical current on the surface of the multi-band antenna. With this technique, the resulted antenna can offer two resonating bands with respect to -10 dB S11. The first band (2.28-2.6) GHz, while the second band (5-5.58) GHz. The proposed antennas have been modeled and simulated using two softwares (CST Microwave Studio and High-Frequency Structure Simulation HFSS) to verify the results of both antennas and the other antenna parameters have been studied by using CST only.*

Keywords-*Sierpinski Curve, Current Distribution Analysis, Dual-band Antenna.*

How to cite this article: M.T. Yassen, "A New Compact Dual-band Antenna Based on Sierpinski Curve Slotted Ground Plane and Current Distribution Analysis," *Engineering and Technology Journal*, Vol. 35, Part A, No. 4, pp. 406-410, 2017.

1. Introduction

Modern wireless applications make the dual band antennas have the vital role of the other types of antennas in many academic and commercial researches. Regarding the slotted antennas, the design of dual-band antenna structure can take three main ways [1]. The first one is to achieve a dual-band resonance frequency depending on two resonators to radiate an electromagnetic wave at two different operating frequencies [2-3]; each of these resonant frequencies of the designed antenna is attributed by each resonator, which has different shape and size. The larger structure will excite the lower resonant frequency and vice versa. The second way includes the excitation another mode by added a reactive load to the structure of a wideband antenna to create a resonance at a second band [4] while the third way denote to splitting the broadband resonance by inserting a notch frequency band [5] to generate a dual bands behavior. A slotted antenna, which has been fed by a microstrip, feed line [6] represents a good example to satisfy the methods mentioned above. It is considered an attractive one because of its simple structure and easy of fabrication. In these types of antennas, slots can take any shape to achieve the purpose of dual band response such as the Euclidean form or fractal shapes as will be explained briefly. Fractal geometries possess two unique properties; space-filling and self-similarity. These properties have essential contributions to find solutions for antennas and electronic in the course of the last three decades. Also, fractals give another era of optimized design tools, initially utilized effectively in antennas but applicable in a general manner [7]. In this respect, the successful application of various fractal geometries to design compact dual-band slot antenna design has been intensively reported in the literature [8-14].

In this paper, an attractive approach to generate a dual-band response from a multi-band antenna has been introduced. The idea of this method is based on changing the path of the electric current from a particular region in the structure of multi-band antenna by using the current distribution analysis to reject an undesired band from the multi-band response.

2. Proposed Multiband Antenna Structure

Figure 1 shows the geometry of the proposed multi-band antenna, which is supposed to be, printed on a compact FR-4 substrate having a relative dielectric constant of 4.4 with dimensions (35.28 × 35.28 × 1.6) mm3. Figure 1(b) represents the front view of the structure which shows the slotted ground plane, the ground plane in the form of a square ring having external dimensions of (Wex × Lex), and internal dimensions of (Win ×

Lin). A Sierpinski curve fractal shape of the first iteration has been employed to the four corners of a small square having dimensions of (Wsq × Wsq) at the middle area inside the ring of the ground plane, each one of them having dimensions equal to the half dimensions of the small square. The proposed multi-band antenna fed by a simple (50) Ω microstrip feed line having dimensions of (Wfl × Lfl) as shown in Figure 1(c).

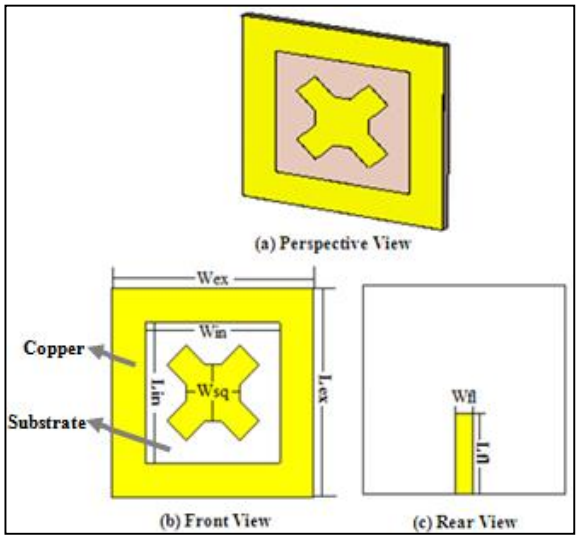

Figure 1: The modeled triple-band antenna structure

The generation process of the Sierpinski curve fractal geometry up to the second iteration is shown in Figure 2 [15]. The square shape in Figure 2(a) represents the starting pattern for this type of fractal. While the generator, which represents the first iteration, is shown in Figure 2(b). The construction of the generator considers four small squares each one of them having dimensions of about half the dimensions of the original one in the previous iteration, has been rotated by (45) degrees and has been placed at each corner of the original square. Then the generator would repeat itself at each corner of a square as a second iteration but with dimensions equal to half the dimensions of the previous iteration and so on.

Table 1 demonstrates the resulting dimensions of the different antenna elements

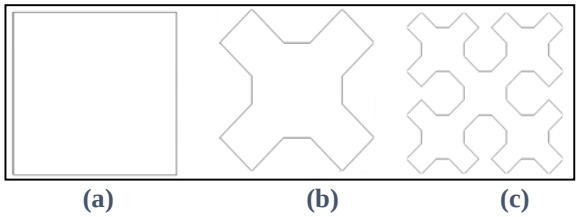

Figure 2: Generation process of the Sierpinski curve fractal geometry

.

Table 1: Summary of the Reference Antenna parameters, in mm

Wex	Lex	Win	Lin
35.28	35.28	23.52	23.52
Wfl	*Lfl*	*Wsq*	
3	13.64	9.4	

3. The Proposed Antenna Design

The current distributions on the surface of the proposed antenna at different frequencies have to be examined, and thoroughly testing relevant antenna parameters have to be checked. Consequently, it has been found that both of the lengths of the internal slot (2×Lin) with the width of it (Win) represent the active parameters on the lower resonance frequency of the designed antenna. In terms of an effective length:

$$Leff = 2 \times Lin + Win \quad (1)$$

Then the lower resonance frequency can be calculated as:

$$f_{RL} \approx \frac{C_o}{Leff \times \sqrt{\varepsilon eff}} \quad (2)$$

4. Performance Evaluation of the Proposed Antenna

Modeling and the performance evaluation of the proposed antennas have been carried out using two EM simulators; the CST Microwave Studio [16], and the High-Frequency Structure Simulation HFSS [17] to verify the results. Figure 3 shows the simulated input reflection coefficient S11 of the modeled antenna. Referring to the CST response and for a swept frequency range from (1-10) GHz, there are three resonating bands. The first band extends from (2.32-2.62) GHz with a center frequency of 2.44 GHz at S11 of -17.12 dB. The second band extends from (4.58-4.96) GHz with a center frequency of 4.77 GHz at S11 of -22.83 dB. The third band extends from (6.42-7.10) GHz with a center frequency of 6.72 GHz at S11 of -25.28 dB.

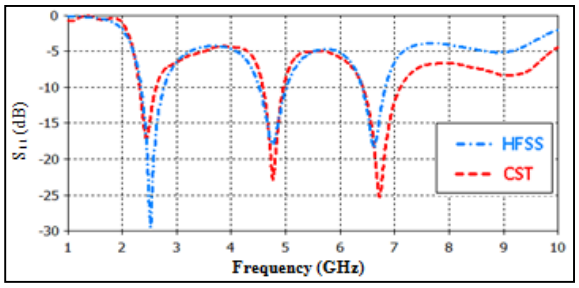

Figure 3: The input reflection coefficient response of the triple-band antenna in CST and HFSS electromagnetic simulators

As described in Equation (1), the current is concentrated around the lower width (Win) of the slot and both of the slot lengths (Lin) as shown in Figure 4(a) and (b). Figure 4 demonstrates the distribution of the current on the surface of the triple band antenna at 2.32 GHz and 2.44 GHz respectively. While the center frequency of the second band in Figure 4(c), the current is concentrated at the internal four corners especially the upper two corners. The structure of the Sierpinski curve shows the current concentration at the center frequency of the third band in Figure 4(d).

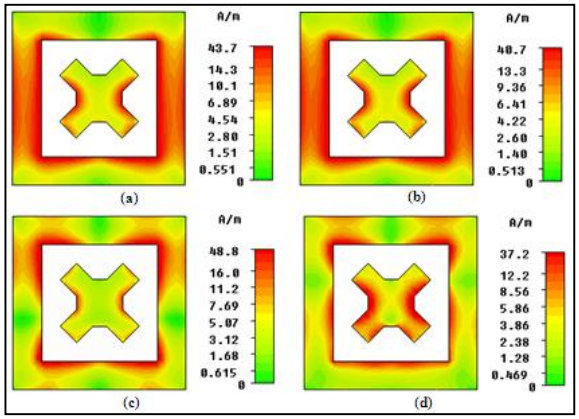

Figure 4: Current distribution analysis on the surface of the triple-band antenna at (a) 2.32 GHz, (b) 2.44 GHz, (c) 4.77 GHz, and (d) 6.72 GHz

5. The Dual-Band Antenna Structure and Performance Evaluation

Since the second band covers the range of frequency extending from (4.58-4.96) GHz and as known there are no applications in this range of frequency. Accordingly, an approach has been studied to remove the middle un-used band from the resonance of Figure 3. This approach is based on current distribution analysis, as the second band depends on the current concentrated at both internal upper corners of the slotted ground plane of the triple-band antenna as shown in Figure 4(c). The current distribution analysis has been found to be an attractive approach in the dual-band and multiband planar antenna design [18]. Then by adding two small squares with dimensions of (4.7×4.7) mm2 to these corners as demonstrated in Figure 5 to control the path of the current, it has been found that the current will change its path resulting to two resonating bands only.

As a result of the above modification of the structure of the triple band antenna, the resulting antenna shows a dual band response in the frequency range from (1-10) GHz in Figure 6. The lower resonating band extends from (2.28-2.6) GHz with a center frequency of 2.42 GHz at S11 of -26.5 dB, and the second resonating band from (5-5.58) GHz with a center frequency of 5.24 GHz at S11 of -28.17 dB.

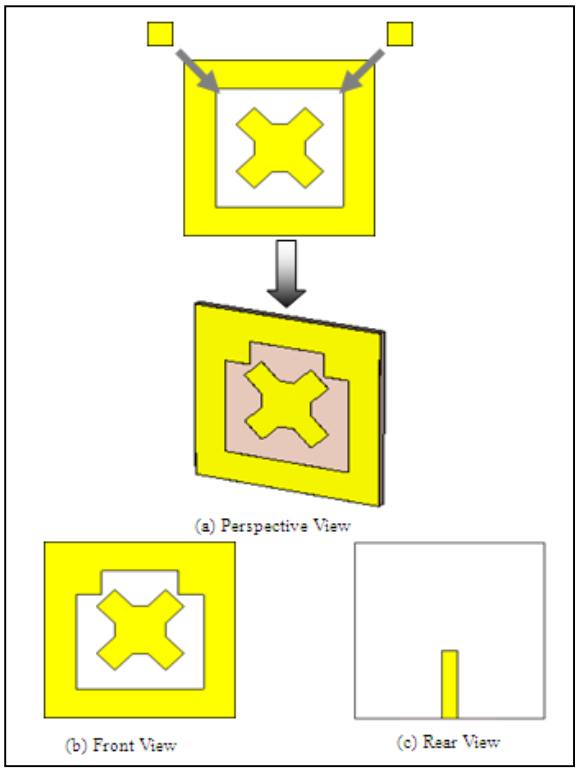

Figure 5: Construction process of the resulting dual-band antenna

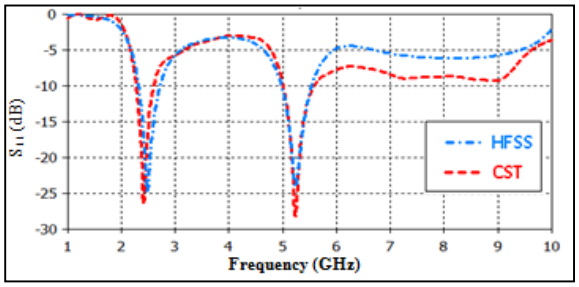

Figure 6: The input reflection coefficient response of the resulting dual-band antenna in CST and HFSS electromagnetic simulators

Figure 7 shows the current distribution analysis at the surface of the resulted dual band antenna. As seen from Figure 4 (a) and (b), the current is focused around the lower width (Win) of the slot and both of the slot lengths (Lin). Figure 7(a) depicts the distribution of the current on the surface of the resulted antenna at the center frequency of the lower band 2.42 GHz. While at the center frequency of the upper band 5.24 GHz in Figure 7(b), the current is focused at the internal two lower corners and around the two squares that have been added to the two inner upper corners. The structure of the Sierpinski curve supports the current concentration at the center frequency of the two resonating bands.

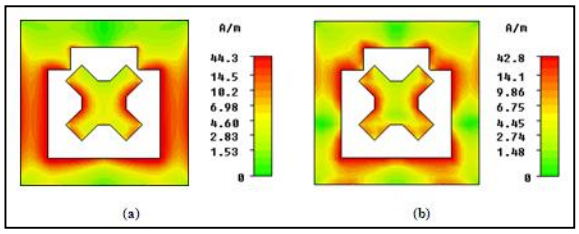

Figure 7: The current distribution on the surface of the dual-band antenna: (a) at 2.42 GHz, and (b) at 5.24 GHz

Figure 8 shows the simulated far–field radiation patterns for the total electric field in the x-y plane, the x-z plane, and the y-z plane at the center frequency of the obtained two bands in this antenna. Figure 8(a) presents the radiation patterns at (2.42) GHz. In the x-y plane ($\theta = 90^o$) the main lobe magnitude is (13.6) dBV/m, the main lobe direction is (180^o), and the angular width (3 dB) is (94.7^o). In the x-z plane ($\varphi = 0^o$) the main lobe magnitude is (17) dBV/m, the main lobe direction is (180^o), and the angular width (3 dB) is (140.8^o). Whereas in the y-z plane ($\varphi = 90^o$) the main lobe magnitude is (17) dBV/m, the main lobe direction is (175^o), and the angular width (3 dB) is (84.8^o). On the other hand, Figure 8(b) demonstrates the radiation patterns at (5.24) GHz. In the x-y plane ($\theta = 90^o$) the main lobe magnitude is (14) dBV/m, the main lobe direction is (-140^o), the angular width (3 dB) is (49.1^o), and the side lobe level is (-2) dB. In the x-z plane ($\varphi = 0^o$) the main lobe magnitude is (16.9) dBV/m, the main lobe direction is (-35^o), the angular width (3 dB) is (129.8^o), and the side lobe level is (-1.4) dB. Whereas in the y-z plane ($\varphi = 90^o$) the main lobe magnitude is (15.9) dBV/m, the main lobe direction is (20^o), the angular width (3 dB) is (60.5^o), and the side lobe level is (-1.1) dB.

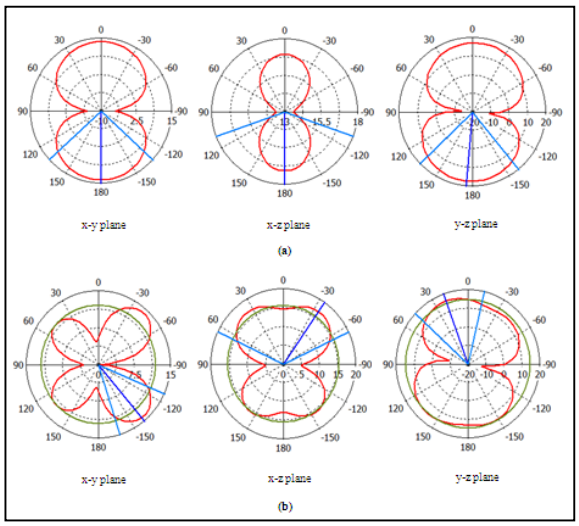

Figure 8: Simulated far–field radiation patterns for the total electric field of the dual band antenna at (a) 2.42 GHz, and (b) 5.24 GHz

The 3D radiation patterns for the total electric field of the resulted dual band antenna are shown in Figure 9. Figure 9(a) shows the 3D radiation pattern corresponding to 2.42 GHz. The results imply that maximum electric field (Emax) equal to 17.04 dBV/m. Figure 9 (b) shows the 3D radiation pattern corresponding to 5.24 GHz, which recorded that maximum electric field (Emax) equal to 16.98 dBV/m. While the values of the peak gain at the two bands are shown as in Figure 10. Throughout the lower resonant band, the peak gain is shown to be as large as 2.27 dBi as demonstrated in Figure 10(a). The upper band gain response is depicted in Figure 10(b). The maximum co-polarization gain of is shown to be of about 2.16 dBi. Furthermore, the peak gain of the resulted antenna is almost unchanged throughout the two resonant bands as illustrated in Figure 10.

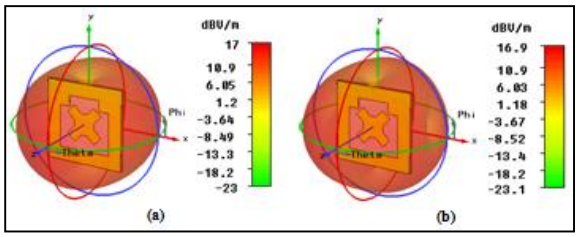

Figure 9: Simulated 3D radiation patterns for the total electric field of the dual-band antenna at (a) 2.42 GHz, and (b) 5.24 GHz

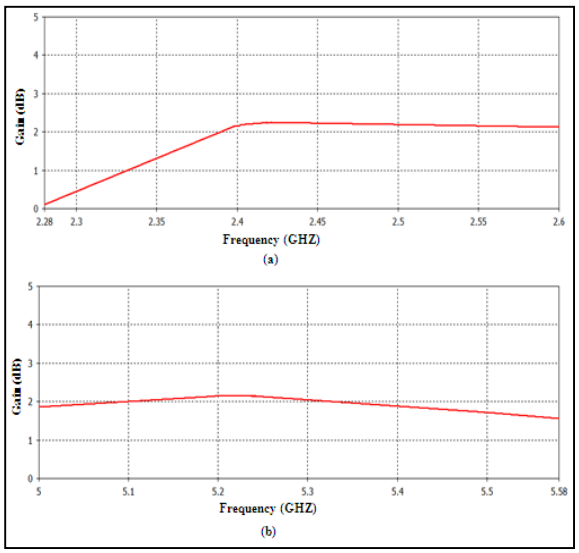

Figure 10: Simulated peak gain of the dual band antenna at (a) 2.42 GHz, and (b) 5.24 GHz

6. Conclusion

A compact slotted ground plane dual – band antenna fed by a simple microstrip feed line has been designed by controlling the path of electric current on the surface of the multi-band antenna. The idea of current distribution analysis proves its capability on rejecting any undesired band from the resonance of any multi-band antenna by modifying its structure to change the path of current away from the regions that responsible on the resonance at the undesired band. The first iteration Sierpinski curve fractal geometry that has been employed to the slotted ground plane of the proposed and the resulted antennas also supports the resonance of these antennas. The resulted antenna offers two resonating bands with acceptable radiation pattern and gain. The lower resonating band ranges from (2.28-2.6) GHz with a center frequency of 2.42 GHz at S11 of -26.5 dB, and the upper resonating band from (5-5.58) GHz with a center frequency of 5.24 GHz at S11 of -28.17 dB. The characteristics of the designed antenna make it suitable for Bluetooth, ISM, RFID, WLAN, 2.5/5.5 WiMax, and WiFi operations.

References

[1] J.K. Ali., S.F. Abdulkareem, A.J. Salim, A.I. Hammoodi, M.T. Yassen, and M.R. Hussan, "Fabrication and Performance Evaluation of a Fractal-based Slot Printed Antenna for Dual-band Wireless Applications," *Iraqi Journal of Computer, Communication and Control Systems Engineering, IJCCCE* , Vol. 14, No. 2, pp. 1-8, 2014.

[2] L. Zhang, T. Jiang, and Y. Li, "Dual-band Printed Antenna for WLAN Applications," Proceedings of Progress in Electromagnetics Research Symposium, Prague Czech Republic, 2015.

[3] P. Zhu, Y-C. Jiao, Y. Zhu, K. Dong, C. Lin, and Q. Zhang, "A Novel Dual-band Monopole Antenna for WLAN Applications," Proceedings of International Symposium on Signals, Systems and Electronics (ISSSE2010), Nanjing, China, 2010.

[4] H.F. Abutarboush, R. Nilavalan, S.W. Cheung, K.M. Nasr, T. Peter, D. Budimir, and H. Al-Raweshidy, "A Reconfigurable Wideband and Multiband Antenna Using Dual-patch Elements for Compact Wireless Devices," *IEEE Transactions on Antennas and Propagation*, Vol. 60, No. 1, pp. 36-43, 2012.

[5] P. Rezaei, M. Hakkak, and K. Forooraghi, "Design of Wide-band Dielectric Resonator Antenna with a Two-segment Structure," *Progress in Electromagnetics Research*, Vol. 66, pp. 111-124, 2006.

[6] P.C. Ooi, and K.T. Selvan, "A Dual-band Circular Slot Antenna with an Offset Microstrip-fed Line for PCS, UMTS, IMT-2000, ISM, Bluetooth, RFID and WLAN Applications," *Progress In Electromagnetics Research Letters*, Vol. 16, pp. 1-10, 2010.

[7] N. Cohen, "Fractal antenna and fractal resonator primer, Chapter 8," in J.A. Rock, and M. van Frankenhuijsen [Eds.], Fractals and Dynamics in Mathematics, Science, and the Arts: Theory and Applications, Vol. 1, World Scientific Publishing Co. Pte. Ltd., Singapore, 2015.

[8] J.K. Ali, S.F. Abdulkareem, A.I. Hammoodi, A.J. Salim, M.T. Yassen, M.R. Hussan and H.M. Al-Rizzo, "Cantor Fractal-based Printed Slot Antenna for Dual-band Wireless Applications," *International Journal of Microwave and Wireless Technologies*, Vol. 8, No. 2, pp. 263-270, 2016.

[9] M.T. Yassen, J.K. Ali, A.J. Salim, S.F. Abdulkareem, A.I. Hammoodi, and M.R. Hussan, "A New Compact Slot Antenna for Dual-band WLAN Applications," *International Journal of Science and Modern Engineering*, Vol. 1, No. 10, pp. 28-32, 2013.

[10] S.F. Abdulkarim, A.J. Salim, J.K. Ali, A.I. Hammoodi, M.T. Yassen, and M.R. Hussan, "A Compact Peano-type Fractal Based Printed Slot Antenna for Dual-band Wireless Applications," Proceedings of 2013 IEEE International RF and Microwave Conference (RFM), , pp. 329-332, Penang, Malaysia, 2013.

[11] J.K. Ali, M.T. Yassen, M.R. Hussan, and A.J. Salim, "A Printed Fractal Based Slot Antenna for Multi-band Wireless Communication Applications," Proceedings of Progress in Electromagnetics Research Symposium, Moscow, Russia. 2012.

[12] J.K. Ali, "A New Microstrip-fed Printed Slot Antenna Based on Moore Space-filling Geometry." Proceedings of IEEE Loughborough Antennas and Propagation Conference, LAPC 2009, pp. 449-452., Loughborough, UK, 2009.

[13] J.K. Ali, and E.S. Ahmed, "A New Fractal Based Printed Slot Antenna for Dual Band Wireless Communication Applications," Proceedings of Progress in Electromagnetics Research Symposium, Kuala Lumpur, Malaysia, 2012.

[14] A.I. Hammoodi, S.F. Abdulkareem, J.K. Ali, A.J. Salim, M.R. Hussan, and M.T. Yassen, "A Circular Cantor Fractal Based Printed Slot Antenna for Triple and Dual-band Wireless Applications," *International Journal of Electronics, Communication and Computer Engineering*, Vol. 4, No. 6, pp. 1707-1712, 2013.

[15] Sierpinski curve Fractal, [Online: Accessed on 3 April 2016]. Available: http://mathworld.wolfram.com / SierpinskiCurve.html

[16] CST, Available [Online]: www.cst.com

[17] HFSS version 11.0, Ansoft Software Inc., 2007.

[18] M.T. Yassen, J.K. Ali, M.R. Hussan, A.J. Salim and H. Alsaedi "Extraction of Dual-band Antenna Response from UWB Based on Current Distribution Analysis," Technical Report, MRG 6–2016, Microwave Research Group, Department of Electrical Engineering, University of Technology, Iraq, March 12, 2016.

Mahmood T. Yassen

M.T. Yassen was born in Basrah, Iraq, in 1978. He received the B.Sc. degree in Communication Engineering from Al-Rasheed College of Science and Technology, Baghdad, Iraq, in 2002 and the M.Sc. degree in Communication Engineering from University of Technology, Baghdad, Iraq, in 2013. Currently, he works in the Electronic Branch, Department of Electrical Engineering, University of Technology, Iraq, as an assistant lecturer. He has published many papers in international conferences and journals in the Fields of microwave antennas and fractal antennas.